PHOTOCATALYTIC ACTIVITY OF BISMUTH VANADATES UNDER UV-A AND VISIBLE LIGHT IRRADIATION: INACTIVATION OF *ESCHERICHIA COLI* VS OXIDATION OF METHANOL

Cristina Adán [a], Javier Marugán [a,*], Sergio Obregón [b], Gerardo Colón [b]

[a] Department of Chemical and Environmental Technology (ESCET), Universidad Rey Juan Carlos, C/Tulipán s/n, 28933 Móstoles (Madrid), Spain.
Tel: +34 91 664 7466, Fax +34 91 488 7068, E-mail: javier.marugan@urjc.es
[b] Instituto de Ciencia de Materiales de Sevilla, Centro Mixto Universidad de Sevilla-CSIC, C/Américo Vespucio, 49, 41092 Sevilla, Spain

Published on
Catalysis Today 240 (2015) 93–99.
doi:10.1016/j.cattod.2014.03.059

ABSTRACT

Four bismuth vanadates have been synthesized by using two different precipitating agents (NH_3 and triethylamine) following a hydrothermal treatment at 100ºC for 2 hours and at 140ºC for 20 hours. Then, solids were characterized by X-ray diffraction, BET surface area, UV–vis spectroscopy and scanning microscopy techniques. The characterization of the synthesized materials showed a well crystallized scheelite monoclinic structure with different morphologies. All materials display optimum light absorption properties for visible light photocatalytic applications. The photocatalytic activity of the catalysts was investigated for the inactivation of *Escherichia coli* bacteria and the oxidation of methanol under UV-vis and visible light irradiation sources. Main results demonstrate that $BiVO_4$ are photocatalytically active in the oxidation of methanol and are able to inactivate bacteria below the detection level. The activity of the catalyst decrease when using visible light, especially for methanol oxidation, pointing out differences in the reaction mechanism. In contrast with bacteria, whose interaction with the catalyst is limited to the external surface, methanol molecules can access the whole material surface.

KEYWORDS: photocatalysis; $BiVO_4$, *Escherichia coli*, methanol, UV-vis, visible.

1. INTRODUCTION

The use of photocatalysis for the destruction of pathogenic microorganism has raised much interest in the environmental applications of this process [1]. Disinfection of bacteria is of particular importance, because traditional methods such as chlorination are chemical intensive and have many associated disadvantages as the well-known generation of chloro-organic byproducts that are highly carcinogenic [2]. So far, TiO_2 is the most widely and most promising photocatalyst used. Its high oxidation capacity, non-toxicity, and high chemical and biological stability are some of the characteristics that make of titanium dioxide superior to other kind of photocatalytic materials. However, in practical applications TiO_2 has been limited for the low utilization of solar energy, responding only to ultraviolet light, which represents a 4 % of the sunlight energy.

Nowadays, new materials having photocatalytic properties are being investigated for their effective utilization of the visible light energy. Generally, these materials are oxides based on metal cations with d^0 or d^{10} configurations, described as AxByOz. These metallates have been reported to take advantage of visible light more efficiently than conventional photocatalysts as TiO_2 [3-5]. Between them, many new visible-light-induced photocatalysts such as AgVOx, Bi_2WO_6, Bi_2MO_6, Bi_2O_3, $CaBi_2O_4$, Bi_5O_7I, $InMO_4$ (M = V, Nb, Ta) or MIn_2O_4 (M = Ca, Sr, Ba) have also been reported [6].

Bismuth vanadate ($BiVO_4$) is one of these visible-light driven semiconductor photocatalysts that has being widely studied due to their steep absorption edges in the visible-light region [7,8]. It is widely accepted that properties of these materials depend on their crystal structure namely as, tetragonal zircon, monoclinic and tetragonal scheelite structures. These crystalline forms can be synthesized by different preparation routes which allow obtaining selectively the mentioned structures depending on the preparation method. However, the most active phase under visible light irradiation reported, seems to be the monoclinic scheelite structure with a band gap of 2,4 eV [6].

Among the variety of methods have been proposed for the preparation of bismuth vanadates, including solid-state reactions, sol–gel method, hydrolysis of metal alkoxides, organometallic decomposition, hydrothermal method and so on, the hydrothermal method has the advantages of allowing the control of the size distribution and particle morphology (sphere-, nanosheet-,

dendrite-, and flower-like) and precipitation can be done from a saturated solution in a single step without any further processing [9]. In addition to that, hydrothermal methodology is a simple and effective pathway in generating monoclinic $BiVO_4$ with perfect crystal structures and regular morphologies [10-12].

$BiVO_4$ has been shown as a promising material for a wide variety of applications, including photocatalytic processes. These materials have been tested in the degradation of dyes [13-15] and others contaminants such as phenol [16], or persistent pollutants such as endocrine disruptors under solar light [17]. Just as many studies about bismuth-based photocatalysts have been focused on degradation of organic pollutants, very few applications have been reported on water disinfection [18,19].

This paper reports the preparation, characterization and photocatalytic activity of four $BiVO_4$ photocatalysts synthesized by a sol-gel method followed by a hydrothermal method. The photocatalytic activity of these materials has been evaluated for the inactivation of *Escherichia coli* and compared to the oxidation of methanol both under UV-visible and visible light irradiation.

2. EXPERIMENTAL

2.1. Synthesis of photocatalysts.

The preparation of $BiVO_4$ was carried out following a procedure previously reported [20]. Briefly, 5 mmol of the Bi precursor was dissolved in 10 mL of glacial acetic acid while the stoichiometric amount of NH_4VO_3 (5 mmol) was dissolved in 60 mL of bidistilled water. These two solutions were finally mixed to form a yellowish suspension (pH = 1 aprox.). Then the pH was settled at 5 by adding NH_4OH or triethylamine (TEA) as pH controlling agent. The resulting suspension was transferred into a Teflon recipient inside of a stainless steel autoclave. The hydrothermal treatment was performed at 100 ºC or 140 ºC for 20 hours. The obtained precipitate was then filtered, repeatedly washed and dried overnight at 120 ºC. Afterwards, thus obtained samples were submitted to a further calcination treatment at 300 ºC for 2 hours. The studied samples will be denoted as N or T for NH_4OH and TEA precipitated series respectively and followed by the hydrothermal treatment temperature.

2.2. Materials characterization.

BET surface area and porosity measurements were carried out by N_2 adsorption at 77 K using a Micromeritics 2010 instrument.

X-ray diffraction (XRD) patterns were obtained using a Siemens D-501 diffractometer with Ni filter and graphite monochromator. The X-ray source was Cu Kα radiation (0.15406 nm). Crystallite sizes for $BiVO_4$ catalysts were estimated from the line broadening of (121) X-ray diffraction signals by using the XPert HighScore Plus software.

The morphology of samples was followed by means of field emission-SEM (Hitachi S 4800). The samples were dispersed in ethanol using an ultrasonicator and dropped on a copper grid. UV–vis spectra were recorded by using a Shimadzu AV2101 in the diffuse reflectance mode (*R*) and transformed to a magnitude proportional to the extinction coefficient (*K*) through the Kubelka–Munk function, $F(R_\infty)$. Samples were mixed with $BaSO_4$ that does not absorb in the UV–vis radiation range (white standard). Scans range was 250–800 nm.

Bismuth and vanadium chemical analysis of the catalysts after reaction was carried out by means of inductively coupled plasma atomic emission spectroscopy (ICP-AES) in a Varian Vista AX equipment. Concentrations were quantified using the spectral lines at 309.310 nm (V) and 306.771 nm (Bi) nm after calibration with certified standards.

2.3. Photocatalytic experiments.

The experimental setup for the photocatalytic reactions consists of an annular reactor 15 cm in lenght, 3 cm inner-tube diameter and 5 cm external-tube diameter operating in a closed recirculating circuit with a stirred reservoir tank. Experiments have been carried out using a catalyst concentration of 0.5 g L^{-1}, a total working volume of 1 L and a recirculation flow rate of 2.5 L min^{-1}. The catalyst concentration was preliminary optimized to ensure full absorption of the incident radiation both with TiO_2 and with the synthesized bismuth vanadates materials. More details about this reactor can be found elsewhere [21].

Illumination was carried out with a 6000 K Xenon car headlight lamp placed in the axis of the

reactor. Spectrum of the light incident to the reactor was controlled with the choice of material for the inner tube of the annulus. Experiments under UV-vis irradiation were carried out using a Pyrex glass tube, whereas visible light driven experiments were performed using a poly-methylmethacrylate (PMMA) inner tube to cut off the light below 380 nm. The radiation flux and spectrum entering the reactor were measured with a BlueWave spectroradiometer (StellarNet Inc.) with a UV–Vis–NIR cosine receptor calibrated in the range 300–1100 nm. Figure 1 shows the comparison betweeen the irradiation spectrum recorded between 300 and 500 nm when glass and PMMA inner tubes were placed in the reactor. As it can be noticed the glass tube keeps almost unaltered the emmision power and spectrum of the unfiltered xenon lamp, whereas PMMA removed most of the UV-A radiation. The integration of the irradiance spectra in the range 276 to 500 nm leads to values of 90 W m^{-2} when using a glass wall and 68 W m^{-2} for the PMMA tube.

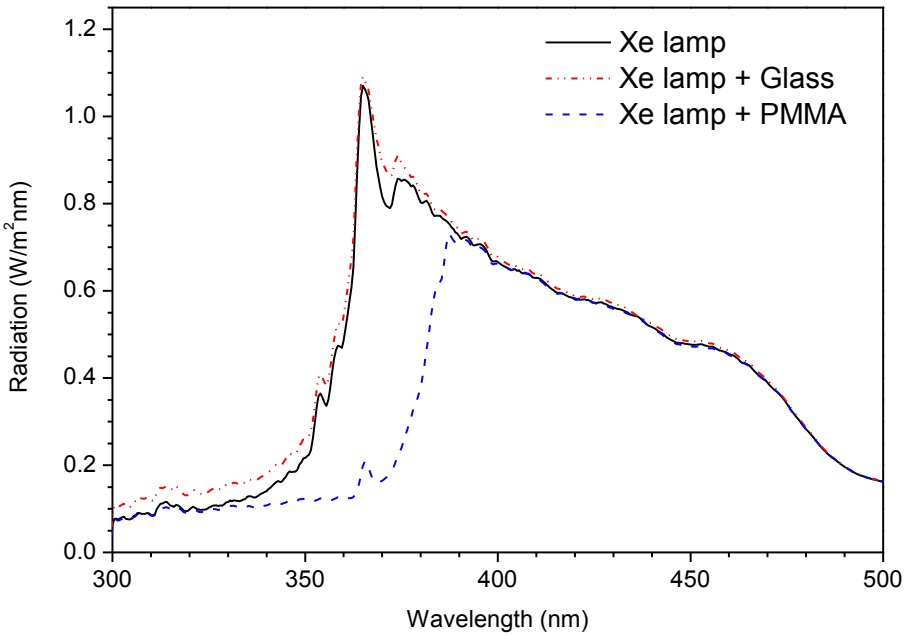

Figure 1. Irradiation spectrums recorded from the Xe lamp without inner tube and using a glass and a poly-methylmetacrilate inner tube.

Bacterial suspensions were prepared from lyophilized *E. coli* K-12 strain samples provided by the Spanish Type Culture Collection (CECT 4624, corresponding to ATCC 23631). Fresh liquid cultures were prepared by inoculation in a Luria–Bertani nutrient medium (Miller's LB Broth, Scharlab) and aerobic incubation at 37 ºC for 24 h under constant rotary shaking. The *E. coli* suspension for the photocatalytic experiments were prepared by rinsing and dilution of

the centrifuged fresh culture to get an initial concentration around 10^6 CFU mL^{-1}. Reactions have been followed by quantifycation of the concentration of viable bacteria by a standard serial dilution method using LB nutrient agar plates (Miller's LB Agar, Scharlab). Eight replicates of each decimal dilution were incubated at 37 ºC for 24 h before counting the number of bacterial colony forming units (CFU). Oxidation of methanol was followed by the formaldehyde formation analysed through a colorimetric method at 412 nm [22]. All experiments have been carried out in deionized water at natural pH and have been repeated twice to test the reproducibility of the results.

Before starting the experiments, the catalyst suspension was stirred and saturated with air for 15 min, being the dissolved oxygen the electron acceptor of the process. In the meantime, the lamp was switched on to stabilize its emission power and spectrum. Measurements of the model pollutants before and after this equilibration time show that adsorption is not significantly detected and can be therefore neglected.

3. RESULTS AND DISCUSSION

According XRD data (Figure 2), the preparation of $BiVO_4$ leads in all cases to well crystallized scheelite structure in the monoclinic phase (PDF 14-0688, corresponding to the *I2/a* space group) [20]. Table 1 summarises the structural and surface features of the synthesised $BiVO_4$ samples. In all cases, the calculated crystallite sizes are in the range of 40-50 nm and the materials exhibit very low BET surface values, in agreement with previous reports [12,23].

Table 1. Characterization of different $BiVO_4$ systems.

Sample	pH controlling agent	Hydrothermal treatment	BET surface area (m^2/g)	Crystallite size (nm)	**Aggregate size (μm)**	Cumulative pore volume (cm^3/g)	Band gap (eV)	SEM Morphology
N5-100	NH_4OH	20h at 100ºC	3	49	10	0.0100	2.39	Peanut-like
N5-140	NH_4OH	20h at 140ºC	3	44	2.5	0.0314	2.38	Peanut-like
T5-100	TEA	20h at 100ºC	3	39	11	0.0264	2.29	Straw-like
T5-140	TEA	20h at 140ºC	1	49	1.7	0.0020	2.35	Polyhedral

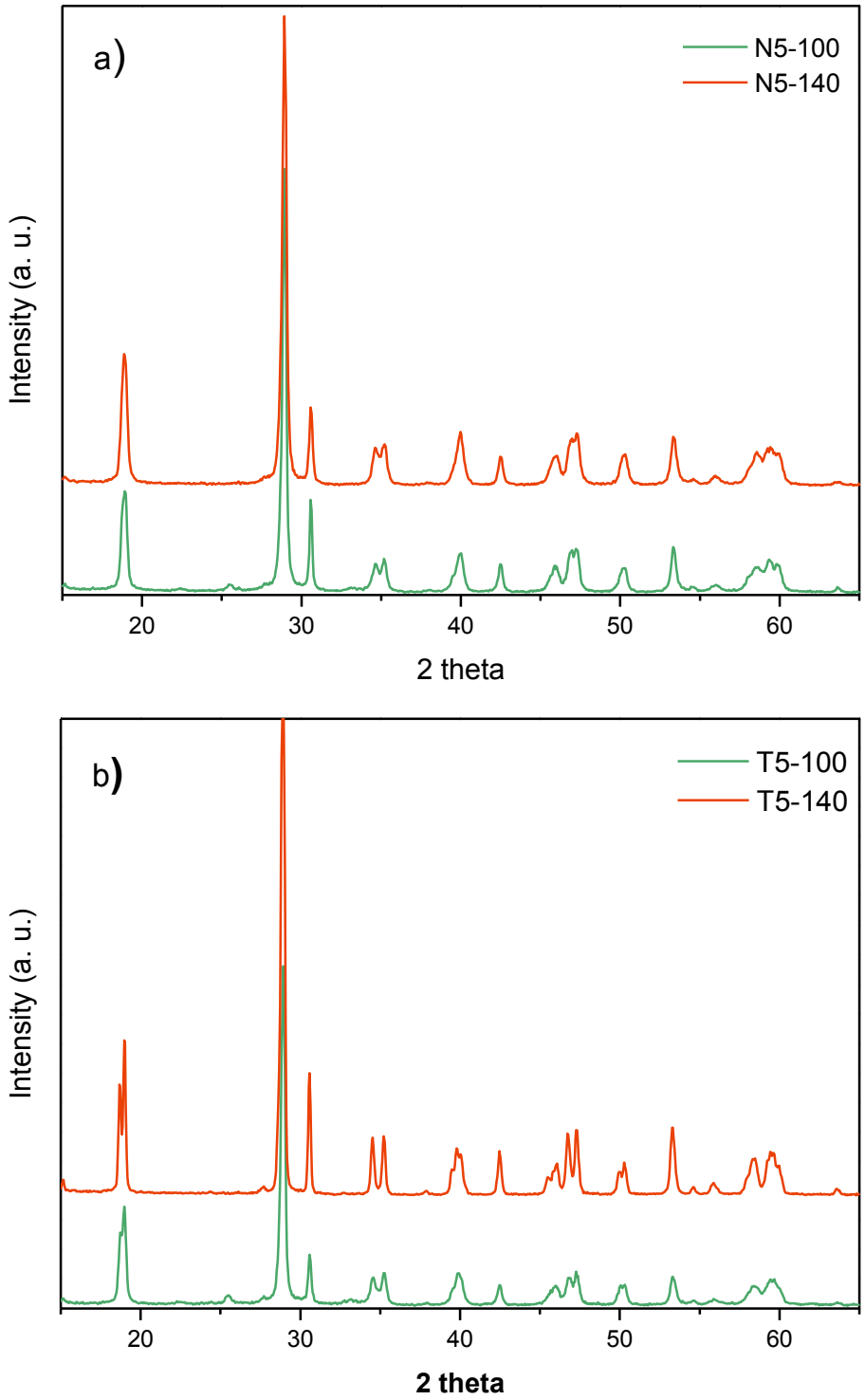

Figure 2. X-ray diffraction patterns for (a) N5 and (b) T5 materials.

As shown in the SEM images of the samples shown in Figure 3, the preparation conditions have significant influence on the morphology of the samples. The $BiVO_4$ prepared at pH = 5 by NH_3 precipitation and hydrothermal treatment at 100ºC shows peanut-like big aggregates of 6-8 µm formed by rounded primary particles (Figure 3a). On the other hand, by using TEA as precipitating agent roundish particles aggregates forming straw-like assembly of about 2-3

μm (Figure 3b) are obtained. The hydrothermal treatment at 140ºC leads, in the case of NH_3 precipitated system, to lower size peanut-like aggregates (Figure 3c). The peanut-like and straw-like particles present microporosity in the nanometer range while for TEA precipitated one, it can be noticed very dense polyhedral particles with lack of porosity as can be appreciable in the micrographs (Figure 2d). This point can be also stated by the significantly low cumulative pore volume obtained for this sample with respect to the rest (Table 1). These results are in agreement with previous studies showing that the different preparation conditions clearly induce dramatic changes in the morphology [24-26]. In this case, these changes with the hydrothermal treatment appear to be more pronounced for samples precipitated by TEA.

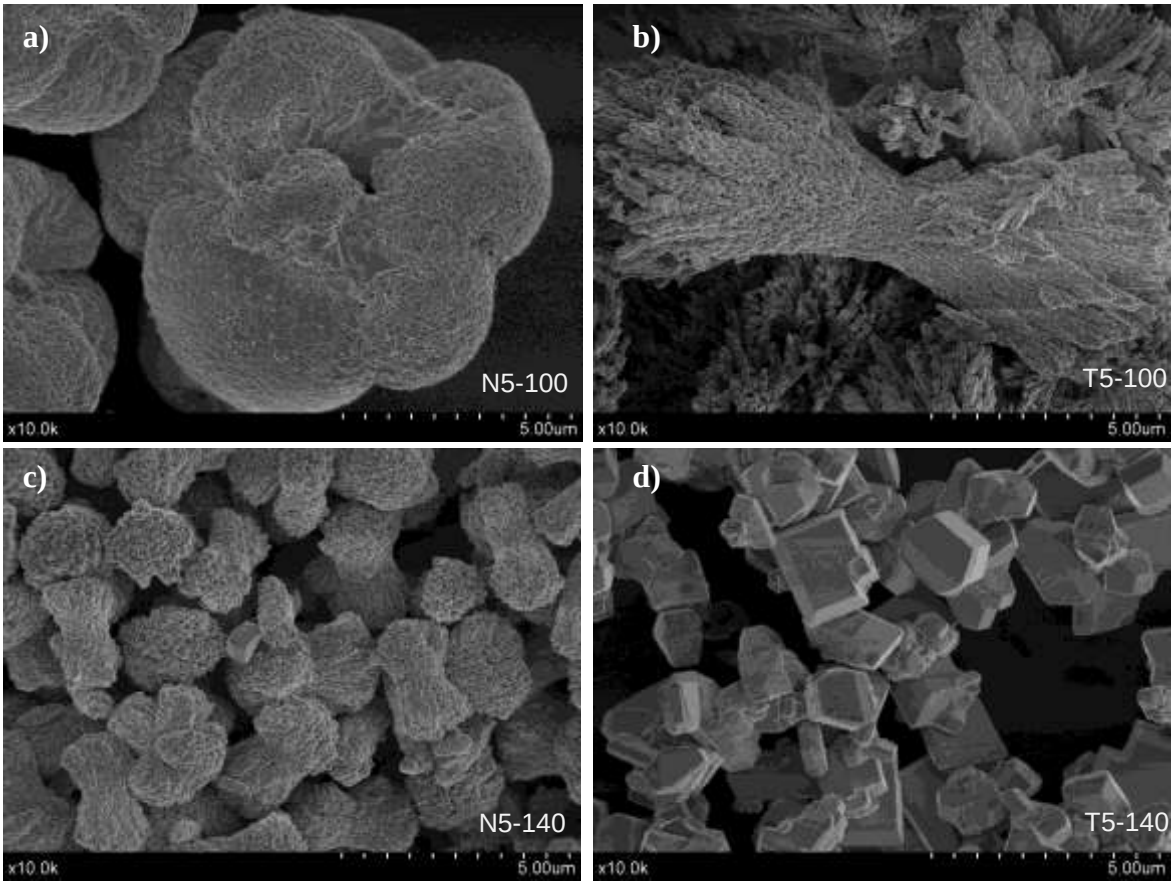

Figure 3. SEM images of the synthesised $BiVO_4$ materials.

The absorption properties of the studied samples were determined by diffuse reflectance UV-visible spectroscopy (Figure 4). $BiVO_4$ obtained by different preparation conditions show similar absorption edge at around 550 nm. This absorption edge corresponds to the

monoclinic structure and leads to calculated band gap values in the range of 2.3-2.4 eV (Table 1), clearly inside the visible range of the spectrum.

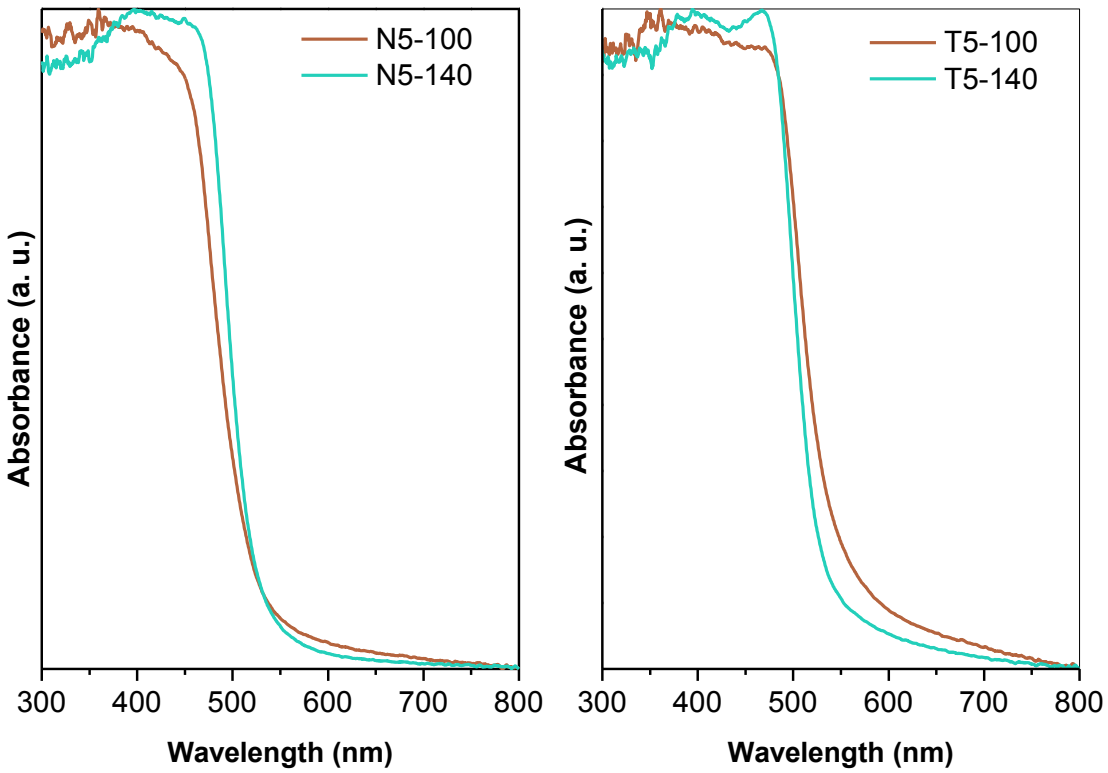

Figure 4. UV-visible diffuse reflectance spectra of the synthesised $BiVO_4$ materials.

The photocatalytic activities of $BiVO_4$ samples were examined in terms of the photocatalytic oxidation of methanol and inactivation of *E. coli* bacteria. The photocatalytic activity of the $BiVO_4$ materials for methanol oxidation has been quantified by fitting the experimental data of formaldehyde formation to a zero-order kinetic equation. This assumption is based on the use of an excess of methanol and that, according to Sun and Bolton [27], the photocatalytic oxidation of methanol under these conditions leads to a quantitative production of formaldehyde. Figure 5 shows the values of the zero-order kinetic constant (k) for formaldehyde production of the different bismuth vanadate samples under UV-visible and visible irradiation. The four $BiVO_4$ catalysts display similar kinetic constants under UV-visible light, while under visible light differences in photocatalytic activity are more noticeable. In general, $BiVO_4$ synthesized with NH_3 exhibit higher visible response than TEA systems although only the N5-100 catalyst exhibits a significant activity. The analysis of bismuth and vanadium lixiviates to the reaction medium after these reactions demonstrate

that catalysts are very stable under the reaction conditions and lixiviation is negligible, being below 0.07% of the V and Bi metal content in all experiments.

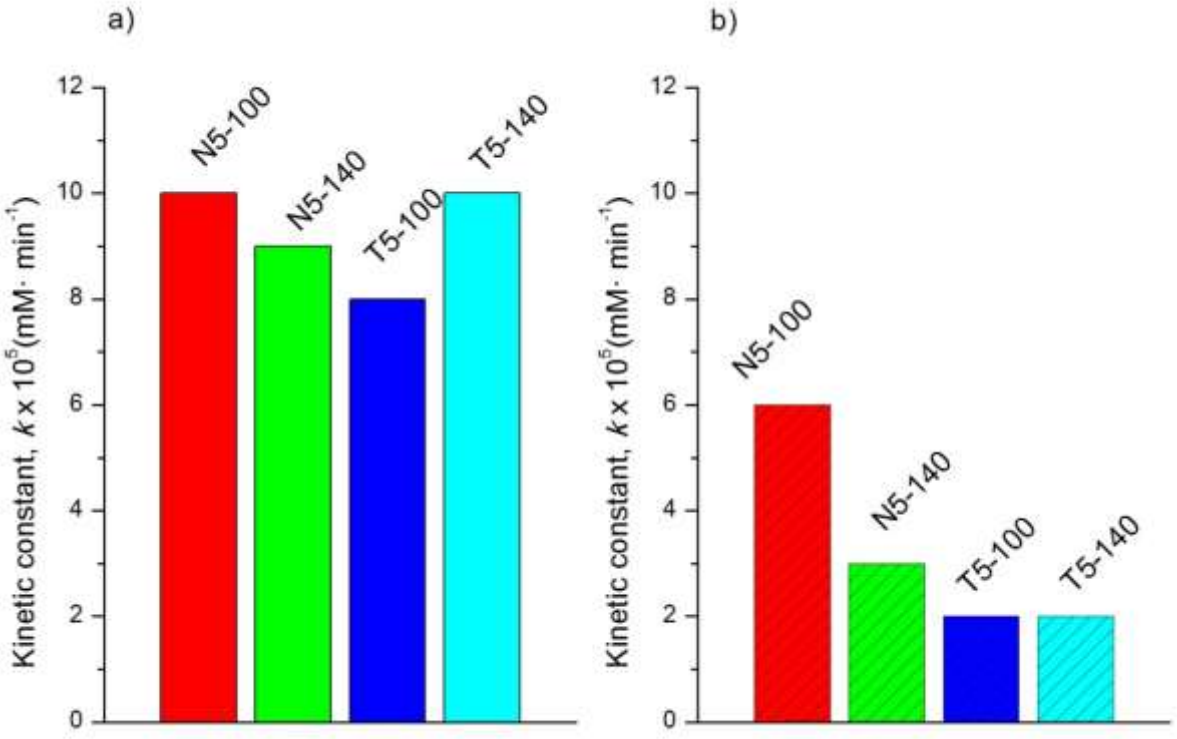

Figure 5. Formaldahyde production rate from methanol photocatalytic oxidation using the studied $BiVO_4$ catalysts under a) UV-Vis and b) visible irradiation. Initial concentration of methanol: 0.1 M.

The comparison of Figure 1 and Figure 4 confirms that there is a good overlapping between the emission spectra of the lamp and the absorption spectra of the catalyst. In both cases, using UV-vis or visible light, the materials should be able to absorb most of the radiation entering the reactor. However, it can be noticed that the decrease in the activity observed when using visible light is significantly more pronounced than the decrease in radiation energy available (90 W m^{-2} with the glass tube and 68 W m^{-2} with the PMMA tube). Consequently, it seems that the reduction in activity of the materials when using visible radiation is not exclusively due to the lower photon absorption in comparison with the use of UV-vis, but to an inherently poorer activity of the material, probably due to the lower oxidation and reduction potential of the electron-hole redox pairs generated under visible irradiation. That could even compromise the possible formation of hydroxyl radicals, leaving

only available the direct hole transfer oxidation mechanism, not really favored in the case of methanol due to its weak adsorption interaction with the catalyst surface.

Regarding the activity for bacterial inactivation, Figure 6 displays the evolution of the concentration of viable *E. coli* bacteria as a function of the irradiation time for samples prepared following hydrothermal treatment at 100ºC. These results confirm the possibility of achieving a six-order of magnitude reduction of CFU concentration and full inactivation of *E. coli* below the bacterial detection limit after few hours of irradiation, with an activity significantly higher than that observed only upon irradiation without the catalyst.

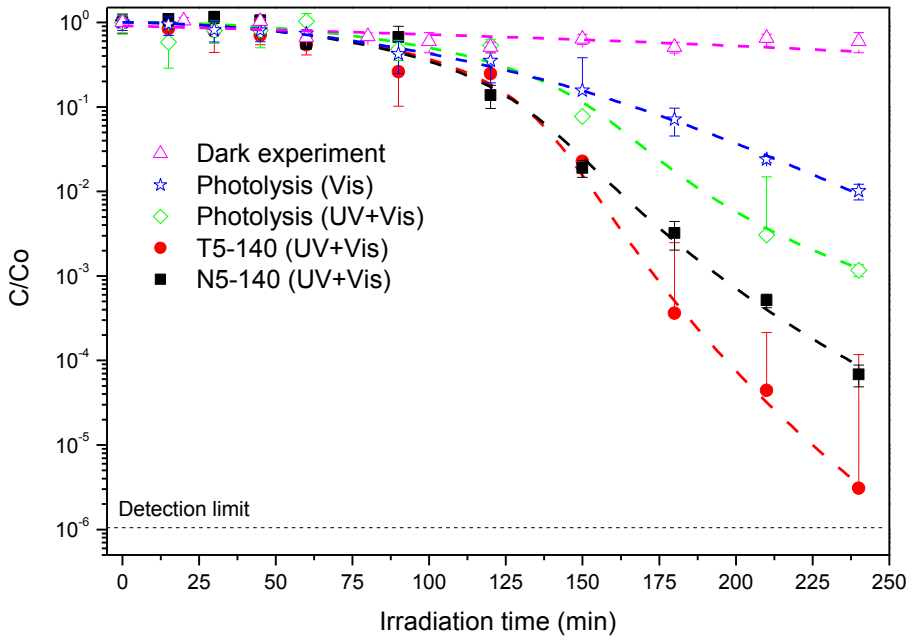

Figure 6. Photocatalytic inactivation of 10^6 CFU mL^{-1} *E. coli* suspensions with N5-140 and T5-140 $BiVO_4$ materials with UV-visible light compared with the control experiments (error bars calculated from eight independent bacteria counting measurements). Dashed lines show the fitting of the experimental data with a kinetic model based on a series event disinfection mechanism [28].

Quantitative results of disinfection activity of the materials have been calculated by fitting the experimental data to a kinetic model based on a series event disinfection mechanism to calculate the inactivation kinetic constant [28]. Results are shown in Figure 7, both for UV-vis and visible irradiation. Under UV-vis irradiation, all $BiVO_4$ materials show *E. coli*

inactivation of more than 4-logs after 4 hours of irradiation. Kinetic constants values for all the catalysts are similar although in this case $BiVO_4$ materials precipitated with TEA display slightly higher values than catalysts precipitated with ammonium. Under visible light irradiation, the T5-140 catalyst seems to show a better response than the rest of the bismuth vanadates. But what is more remarkably is that in this case the decrease in the activity under visible light in comparison with the activity under UV-vis is not as pronounced as it was for the photocatalytic oxidation of methanol. Reduction in the efficiency is consistent with the decrease in irradiation power suggesting that in this case no change in mechanism is observed depending of the wavelength range of irradiation.

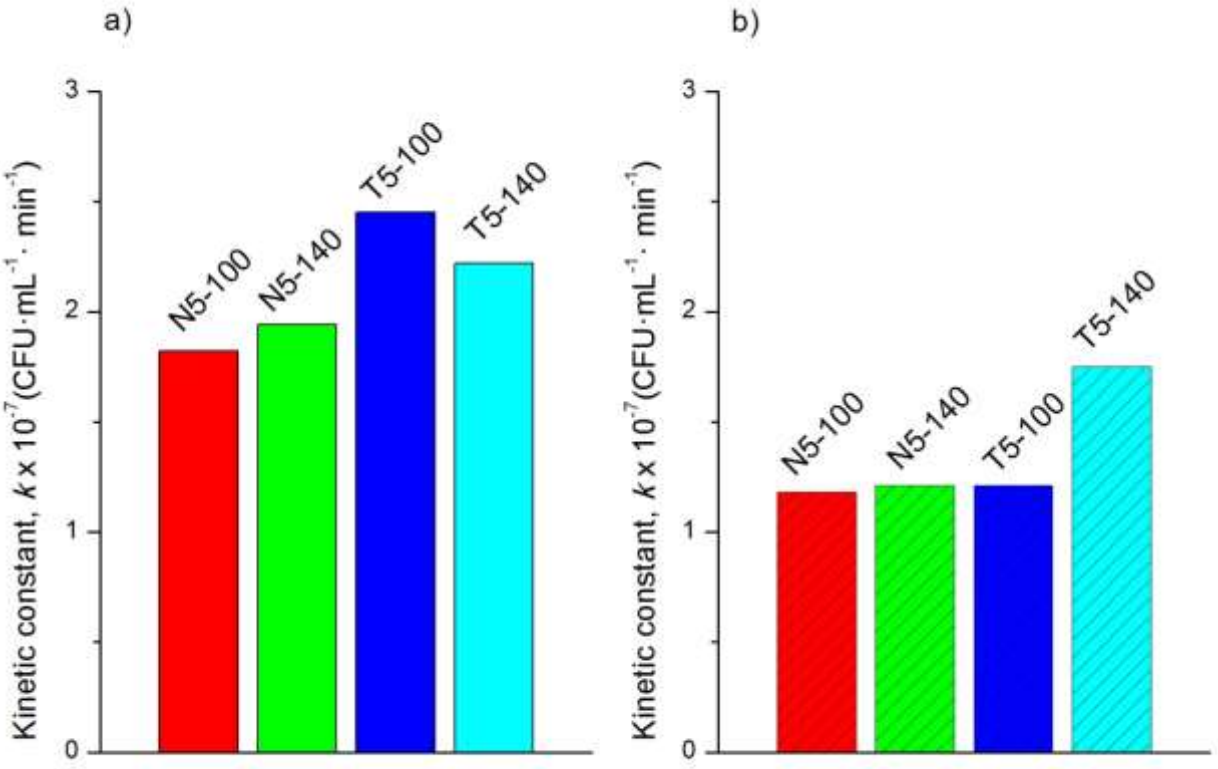

Figure 7. Influence of $BiVO_4$ catalysts on the kinetic constants for inactivation of 10^6 CFU mL^{-1} *E. coli* suspensions obtained under a) UV-vis and b) visible irradiation. Initial concentration of methanol: 0.1 M.

The comparison between methanol and *E. coli* studies allows understanding which effects are exclusively due to the photoactivation of the catalyst and those related to the microbiological aspects of the disinfection processes. First, it can be noted that all bismuth vanadates display

a good photocatalytic response both by using the full UV-vis spectrum of the Xe-lamp and only visible light. Moreover, all $BiVO_4$ materials exhibit similar kinetic constants under UV-vis irradiation, in accordance with their similar physicochemical properties. However, slight differences in the kinetic constants become more remarkable when using only visible light. Those results are difficult to explain based on physicochemical data, as the small differences observed in band gap values, crystal particle size or surface area are not enough to explain the best activity observed in the N5-100 catalyst. Some authors have associated the different activity behaviour of bismuth vanadates, having the same crystal structure, with the particle morphology which in turn affect the properties of these materials [13,23,29,30]. Thereby, Fan et al. [23] studied the different morphologies of monoclinic $BiVO_4$ samples and they observed that the flower-like $BiVO_4$ particles exhibit a high photocatalytic performance which was related with a high separation efficiency of photo-carriers. The lamellar $BiVO_4$ particles reported by Ke et al [31] also showed the best photocatalytic activity for O_2 evolution. As them, other authors have related the photocatalytic activity of $BiVO_4$ samples to the particles morphologies [24,32]. In this case, peanut-like $BiVO_4$ particles present better photocatalytic results under visible light. These materials seem to favor higher visible light absorption and/or lower recombination process.

However, two factors should be taken into account when comparing the results obtained with bacteria and organic molecules. One of them is related to the interaction between catalyst and methanol or catalysts and bacteria. For an effective photocatalytic degradation process, the direct contact between pollutants and photocatalysts is very important but in the case of microorganisms, the inactivation by h^+ and •OH radicals required close contact between the catalyst and the bacteria [19,33]. It is widely accepted that to reach bacterial inactivation is necessary to achieve a number of cumulative •OH radical attacks to disrupt the cell wall. Therefore, it is expected that catalyst under visible light conditions take longer to reach the amount of cell damage necessary for bacterial inactivation, as it is confirmed in Figure 7. But, in any case, this mechanism implies a good contact between the bacterium membrane and surface catalyst. On the other hand, this catalyst surface/bacteria interaction can be influenced by the catalysts charge surface. It is known that the point of zero charge of $BiVO_4$ is around 2.5 [14,34]. This would indicate that in the reaction media, the $BiVO_4$ surface might be negatively charged. The importance of pollutant adsorption over the negatively charged $BiVO_4$ surface has been previously stated for rhodamine B and methylene blue [35]. In the present case, methanol adsorption won't be favoured, whereas electrostatic repulsion with the

negatively charged bacteria surface would be produced unless an intermediate counter ion layer of cations is formed, favouring the interaction with the catalyst surface as suggested by Pablos et al. [36]. Assuming that the under visible light hydroxyl radical formation is hindered and short-distance hole transfer could be favored, this fact could explain why the decrease in the activity when using visible light is more pronounced for methanol oxidation than for *E. coli* inactivation.

The second factor that can affect the photocatalytic response of bismuth vanadates is the aggregate size and porosity of the materials (Table 1). Although all catalysts present low BET surface areas, the porosity of the catalysts depend on the preparation conditions (Figure 3). Chemicals can diffuse through the porosity and access deeper active sites inside of the catalysts particle, reaching a larger extension of surface area of the $BiVO_4$, which is more notable for porous peanut-like and acicular particles. However, in the case of *E. coli* inactivation due to its huge size only the most external surface of the $BiVO_4$ particles is really available for the interaction with the bacteria. This fact can explain why the T5-140 catalyst, being one of the least porous catalysts and showing the smallest aggregate size, can show the highest photocatalytic activity. Thus, it can be assumed that the external surface and an intimate contact favoured by the smaller particle size can play an important role in the bacteria inactivation. However, the opposite behavior is not necessarily observed, showing the most porous materials not always the highest activities for methanol oxidation.

4. CONCLUSIONS

In summary, all the studied $BiVO_4$ materials have proved to be active under UV-visible and visible light irradiation, with only slightly different kinetic constants both for the photocatalytic oxidation of methanol and the inactivation of *E. coli*. Catalysts prepared with NH_3 display better photocatalytic response in the degradation of methanol whereas in the case of inactivation of bacteria the more active catalyst are $BiVO_4$ materials prepared with TEA. In both types of reaction, kinetic constants decrease when using visible light in comparison the use the full spectrum of UV-vis light of the Xe-lamp. However, whereas the decrease in the activity for the inactivation of bacteria is more or less in agreement with the reduction in the total radiation power, the decrease in the efficiency for methanol oxidation is much more significant, pointing out differences in the reaction mechanism in addition to

lower radiation absorption. In contrast with bacteria, whose interaction with the catalyst is limited to the external surface, methanol molecules can access the whole material surface.

ACKNOWLEDGEMENTS

The authors gratefully acknowledge the financial support of the Spanish Ministry of Economy and Competitiveness (MINECO) through the project EMBIOPHOTO (CTM2011-29143-C03-01), Comunidad de Madrid through the program REMTAVARES (S2009/AMB-1588) and Junta de Andalucía through the Excellence project FQM-4570. C. Adán is indebted to the MINECO for its Juan de la Cierva postdoctoral contract (JCI-2010–06430). S. Obregón thanks for his JAE-Pre grant.

REFERENCES

[1] P.K.J. Robertson, J.M.C. Robertson, D.W. Bahnemann, J. Hazard, Mater 211 (2012) 161-171.

[2] P.S.M. Dunlop, J.A. Byrne, N. Manga, B.R. Eggins, J. Photochem. Photobiol. A:Chem. 148 (2002) 355-363.

[3] E. Gkika, P. Kormali, S. Antonaraki, D. Dimoticali, E. Papaconstantinou, A. Hiskia, Int. J. Photoenergy 6 (2004) 227-231.

[4] C. Belver, C. Adán, M. Fernández-García, Catal. Today 142 (2009) 274-281

[5] C. Belver, C. Adán, S. García-Rodríguez, M. Fernández-García, Chem Eng. J. 224 (2013) 24-31.

[6] A. Kubacka, M. Fernández-García, G. Colón, Chem. Rev. 112 (2012) 1555-1614.

[7] W.Z. Yin, W.Z. Wang, L. Zhou, S.M. Sun, L. Zhang, J. Hazard. Mater. 173 (2010) 194-199.

[8] X. Zhang, L. Dua, H. Wang, X. Dong, X. Zhang, C. Ma, H. Ma, Micropor. Mesopor. Mater. 173 (2013) 175-180.

[9] Y. Guo, X. Yang, F. Ma, K. Li, L. Xu, X. Yuan, Y. Guo. Appl. Surf. Sci. 256 (2010) 2215-2222.

[10] J. Yu, A. Kudo, Adv. Funct. Mater. 16 (2006) 2163–2169.

[11] L. Zhou, W. Wang, S. Liu, L. Zhang, H. Xu, W. Zhu, J. Mol. Catal. A Chem. 252 (2006) 120-124.

[12] A. Zhang, J. Zhang, N. Cui, X. Tie, Y. An, L. Li, J. Mol. Catal. A Chem. 304 (2009) 28-32

[13] J. Zhang, W. Luo, W. Li, X. Zhao, G. Xue, T. Yu, C. Zhang, M. Xiao, Z. Li, Z. Zou, Electrochem. Comm. 22 (2012) 49-52.

[14] B. Xie, H. Zhang a, P. Cai, R. Qiu, Y. Xiong, Chemosphere 63 (2006) 956-963.

[15] L. Ge, Mater. Chem. Phys. 107 (2008) 465-470.

[16] Z. Zhang, W. Wang, M. Shang, W. Yin, Catal. Comm. 11 (2010) 982-986.

[17] S. Kohtani, M. Koshiko, A. Kudo, K. Tokumura, Y. Ishigaki, A. Toriba, K. Hayakawa, R. Nakagaki, Appl. Catal. B: Environ. 46 (2003) 573-586.

[18] H. Gan, G. Zhang, H. Huang, J. Hazard. Mater. 250 (2013) 131-137.

[19] W. Wang, Y. Yu, T. An, G. Li, H.Y. Yip, J.C. Yu, P.K. Wong, Environ. Sci. Technol. 46 (2012) 4599-4606.

[20] S. Obregón, A. Caballero, G. Colón, Appl. Catal. B: Environ. 117-118 (2012) 59- 66.

[21] R. van Grieken, J. Marugán, C. Sordo, C. Pablos, Catal. Today 144 (2009) 48-54.

[22] T. Nash, Biochem. J. 55 (1953) 416-421.

[23] H. Fan, D. Wang, L. Wanga, H. Li, P. Wang, T. Jiang, T. Xie, Appl. Surf. Sci. 257 (2011) 7758-7762.

[24] Y. Zhao, Y. Xie, X. Zhu, S. Yan, S. Wang, Chem. Eur. J. 14 (2008) 1601-1606.

[25] L. Zhou, W. Wang and H. Xu, Cryst. Growth Des. 8 (2008) 728-733.

[26] M. Shang, W. Wang, J. Ren, S. Sun, L. Zhang, Cryst. Eng. Comm. 12 (2010) 1754-1758.

[27] L. Sun, J.R. Bolton, Determination of the quantum yield for the photochemical generation of hydroxyl radicals in TiO2 suspensions. J. Phys. Chem. 100 (1996) 4127.

[28] J. Marugán, R. van Grieken, C. Sordo, C. Cruz, Appl. Catal. B: Environ. 82 (2008) 27-36.

[29] M. Zhang, C. Shao, P. Zhang, C. Su, X. Zhang, P. Liang, Y. Sun, Y. Liu. J. Hazard. Mater. 225-226 (2012) 155-163.

[30] Y. Guo, X. Yang, F. Ma, K. Li, L. Xu, X. Yuan, Y. Guo. Appl. Surf. Sci. 256 (2010) 2215-2222.

[31] D. Ke, T. Peng, L. Ma, P. Cai, K. Dai, Inorg. Chem. 48 (2009) 4685-4691.

[32] F.X. Wang, M.W. Shao, L. Cheng, J. Hua, X.W. Wei, Mater. Res. Bull. 44 (2009) 1687-1691.

[33] C. Pablos, R. van Grieken, J. Marugán, I. Chowdhury, S.L. Walker, Catal. Today 209 (2013) 140-146.

[34] N.C. Castillo, L. Ding, A. Heel, T. Graule, C. Pulgarín, J. Photochem. Photobiol. A:Chem. 216 (2010) 221-227.

[35] S. Obregón, G. Colón, J. Mol. Catal. A: Chem. 376 (2013) 40-47.

[36] C. Pablos, R. van Grieken, J. Marugán, I. Chowdhury, S.L. Walker, Catal. Today 209 (2013) 140-146.